

000 RELIGHTMASTER: PRECISE VIDEO RELIGHTING 001 002 WITH MULTI-PLANE LIGHT IMAGES 003 004

005 **Anonymous authors**

006 Paper under double-blind review

007 008 ABSTRACT 009

010 Recent advances in diffusion models enable high-quality video generation and
011 editing, but precise relighting with consistent video contents, which is critical for
012 shaping scene atmosphere and viewer attention, remains unexplored. Mainstream
013 text-to-video (T2V) models lack fine-grained lighting control due to text’s inherent
014 limitation in describing lighting details and insufficient pre-training on lighting-
015 related prompts. Additionally, constructing high-quality relighting training data is
016 challenging, as real-world controllable lighting data is scarce. To address these is-
017 sues, we propose RelightMaster, a novel framework for accurate and controllable
018 video relighting. First, we build RelightVideo, the first dataset with identical dy-
019 namic content under varying precise lighting conditions based on the Unreal En-
020 gine. Then, we introduce Multi-plane Light Image (MPLI), a novel visual prompt
021 inspired by Multi-Plane Image (MPI). MPLI models lighting via K depth-aligned
022 planes, representing 3D light source positions, intensities, and colors while sup-
023 porting multi-source scenarios and generalizing to unseen light setups. Third, we
024 design a Light Image Adapter that seamlessly injects MPLI into pre-trained Video
025 Diffusion Transformers (DiT): it compresses MPLI via a pre-trained Video VAE
026 and injects latent light features into DiT blocks, leveraging the base model’s gener-
027 ative prior without catastrophic forgetting. Experiments show that RelightMaster
028 generates physically plausible lighting and shadows and preserves original scene
029 content.

030 1 INTRODUCTION

031 With the advancement of video generation technology (Blattmann et al., 2023; Wan et al., 2025),
032 it is now possible to generate high-quality, long video clips comparable to movies. Improving the
033 controllability of video generation is a pressing need for downstream applications, e.g., camera tra-
034 jectory control (Bian et al., 2025; He et al., 2025) and multi-identity preservation (Liu et al., 2025a).
035 As a fundamental element of video content creation, lighting plays an irreplaceable role: it shapes
036 the visual atmosphere of scenes, enhances spatial depth, and guides viewers’ attention—directly
037 determining the aesthetic and communicative effect of video content. However, achieving precise
038 lighting control and flexible lighting editing remains highly challenging. Traditionally, professional
039 video lighting relied on specialized equipment or specific environmental conditions, which are dif-
040 ficult for ordinary creators to replicate. Even with the lowered creation threshold brought by video
041 generation models, mainstream text-to-video (T2V) models still fail to support accurate, fine-grained
042 lighting control, creating a critical gap between technical capability and practical demand. We pro-
043 pose a framework RelightMaster for precise video relighting.

044 We observe that there are two core challenges hindering the progress of video relighting. First,
045 constructing high-quality training data for relighting is extremely difficult. Real-world video data
046 with controllable lighting conditions is scarce: adjusting lighting parameters in physical scenes is
047 time-consuming, costly, and unable to ensure consistent content across different lighting setups. To
048 mitigate this, we turn to game engines (e.g., Unreal Engine 5 (Games, 2022)) to generate synthetic
049 data. Nevertheless, such synthetic data still has limitations: its appearance (e.g., texture details,
050 color realism) differs significantly from general real-world video data, and the limited data volume
051 easily leads to model overfitting. This calls for an effective method to activate the prior knowledge
052 already learned by pre-trained video generation models, bridging the gap between synthetic and
053 real data. Second, representing and inputting lighting information accurately is a bottleneck. T2V

models primarily take text prompts as input, but text is inherently inadequate for describing fine-grained lighting details (e.g., light position, intensity distribution, color temperature). Worse still, the prompts used in T2V pre-training rarely include lighting-related descriptions, leaving models unable to learn effective lighting representations from text, which further limits the precision of lighting control. To address this challenge, we argue that a visual prompt is needed: one that can not only provide precise, quantitative control signals for light sources (e.g., positional and intensity information) but also naturally align with the video prior (i.e., the visual distribution and spatial structure learned by pre-trained video generation models), thus overcoming the inaccuracy of text-based lighting control while leveraging existing model knowledge.

We draw inspiration from the multi-plane image (MPI) (Tucker & Snavely, 2020) representation and propose a novel Multi-plane Light Image (MPLI) for video relighting. The core idea of MPLI is to model lighting information in a spatially aligned manner with video content: we first extract K depth planes from the camera frustum, covering the spatial hierarchy of the scene. Then, we calculate the irradiance on each of these K planes based on the 3D position of the light source, generating K corresponding Light Images. This design endows MPLI with three key advantages: (1) it fully captures the 3D positional information of light sources, establishing a natural alignment with the 2D frame modality of video; (2) it inherently supports multi-light-source scenarios. Multiple light sources can be integrated by superimposing their respective irradiance calculations on the K planes; (3) it exhibits strong generalization: in our experiments, even when trained only on single-light-source data, the model naturally supports multi-light-source relighting, verifying the robustness of the MPLI.

To seamlessly integrate MPLI as a control condition into existing video generation models, we further propose a Light Image Adapter. Current video generation models typically use a Video Variational Autoencoder (VAE) to compress K video frames into a single video latent feature, which is then processed by a patchify module and fed into a Diffusion Transformer (DiT) (Peebles & Xie, 2023) for generation. To align MPLI with the visual distribution learned by the diffusion model, we first compress the K Light Images of MPLI into a single latent light feature using the same pre-trained Video VAE. The Light Image Adapter is initialized with parameters from the pre-trained patchify module, which ensures consistency with the model’s prior knowledge, and injects the latent light feature into the network before each DiT block. This lightweight integration not only preserves the original generation capability of the DiT model but also enables precise, fine-grained control over video relighting. In contrast, previous methods (Zhou et al., 2025; Zhang et al., 2024) only relit videos with rough texts or replace the background with environment maps.

The main contributions of our work can be summarized as follows:

- We propose a novel light representation, the Multi-plane Light Image (MPLI), that explicitly encodes the spatial properties of 3D light sources and aligns naturally with the video modality. The MPLI enables dynamic multisource light control and demonstrates strong generalization.
- We propose a lightweight and efficient Light Image Adapter that seamlessly injects the MPLI condition into pre-trained Video DiT models. This allows for precise lighting control while leveraging the vast generative prior of the base model, avoiding catastrophic forgetting and the need for full retraining.
- We build a dataset, RelightVideo, the first video dataset that renders the same dynamic contents with different lighting conditions, advancing the cutting-edge research on light control in video generation and editing.
- We propose a novel framework, RelightMaster, for accurate and controllable video relighting that generates physically plausible lighting and shadow effects across the entire scene while preserving the original background content.

2 RELATED WORKS

Diffusion Models for Relighting. Traditional image relighting methods rely on intrinsic image decomposition (Luo et al., 2020; Careaga & Aksoy, 2023; Liang et al., 2025), which decomposes an sRGB image into shading, albedo, and then replaces the shading according to the estimated normals. Recently, text-to-image (T2I) diffusion models (Dhariwal & Nichol, 2021; Ho et al., 2020;

108 Rombach et al., 2022; Song et al., 2020) have emerged as pivotal foundational models in image
 109 editing, attributed to their strong capability in learning real-world image priors. For the task of
 110 image relighting, a prominent approach is fine-tuning these pre-trained T2I models. Such methods
 111 eliminate the need for explicit decomposition of intrinsic scene components (e.g., shape, albedo) and
 112 directly leverage the learned priors of lighting and scene consistency to achieve flexible and realistic
 113 illumination editing, supporting diverse control modalities like text descriptions and environment
 114 maps. Representative works include LightIt (Kocsis et al., 2024), DiLightNet (Zeng et al., 2024),
 115 IC-Light (Zhang et al., 2024), and LightLab (Magar et al., 2025) . Recently, Light-A-Video (Zhou
 116 et al., 2025), TC-Light (Liu et al., 2025b), and RelightVid (Fang et al., 2025) extend the image
 117 relighting method IC-Light to video relighting. **Lumen (Zeng et al., 2025) replaces the background**
 118 **in videos while correspondingly adjusting the lighting in the foreground with harmonious blending.**
 119

120 **Diffusion Models for Video Editing.** Diffusion-based video generation techniques have also under-
 121 gone remarkable advancements (Blattmann et al., 2023; Wan et al., 2025; Singer et al., 2025; Ling
 122 et al., 2024). Leveraging these developments, training-free paradigms including AnyV2V (Ku et al.,
 123 2024), MotionClone (Ling et al., 2024), and BroadWay (Bu et al., 2024) facilitate prompt-guided op-
 124 erations such as inpainting, style transfer, and motion retargeting without requiring additional model
 125 fine-tuning. For achieving frame-level consistency in edited content, fine-tuning-based approaches
 126 like ConsistentVideoTune (Cheng et al., 2023) and Tune-A-Video (Wu et al., 2022) adapt pre-trained
 127 video diffusion models to user-provided references, enabling seamless object insertion and consis-
 128 tent color grading effects. Recently, a series of video relighting methods (Zhou et al., 2025; Liu
 129 et al., 2025b; Fang et al., 2025) extend IC-Light (Zhang et al., 2024) from image relighting to video
 130 relighting. All of the three methods inherent the nature of IC-Light: most lighting controllability
 131 comes from the environment map instead of the input text. However, once using the environment
 132 map, it requires handcrafting the foreground objects for relighting and enforces static background
 133 replacement based on provided environment maps, which does not meet the requirements of video
 134 relighting under general circumstances. Camera trajectory editing (Bian et al., 2025; He et al., 2025;
 135 Gu et al., 2025; Bai et al., 2025) can be regarded as a type of video editing. Inspired by ReCamMas-
 136 ter (Bai et al., 2025) that synthesized video pairs that share the same dynamic contents via graphics
 137 engines, we propose RelightMaster that learns relighting from rendered video pairs. In contrast to
 138 previous video relighting methods (Zhou et al., 2025; Liu et al., 2025b; Fang et al., 2025), our pro-
 139 posed RelightMaster achieves good light control with end-to-end generation while preserving the
 140 complete original video content.

3 DATASET

143 Collecting video pairs with varying lighting conditions in the real world is challenging. Setting
 144 up lighting in real scenes is time-consuming and expensive, which limits the data diversity and
 145 scalability. For example, light stages commonly used to collect 3D human body data often feature
 146 monotonous backgrounds. Even worse, it is difficult to ensure that the dynamic objects remain
 147 consistent across multiple video recordings. Using synthetic data can effectively circumvent the
 148 problem of inconsistent motion, and advanced game engines can provide extremely realistic lighting
 149 simulations at a low cost.

150 We build a dataset rendering pipeline based on Unreal Engine to batch generate video training data
 151 with the same content but different lighting. We collected 24 3D scene assets as static backgrounds
 152 and randomly bound 93 actions to 66 human models as dynamic object foregrounds. Finally, we ob-
 153 tained 652 assembled scenes after random combination. Fig. 1 presents an overview of our dataset.
 154 For each scene, we use four random camera trajectories centered on dynamic objects to render the
 155 original video, that is, the reference video without changing the lighting conditions. We then add
 156 additional point lights with randomized parameters to the existing scene and render the target video
 157 again with the changed lighting conditions. We adjust the 3D position, color, and intensity of the
 158 point lights to provide fine-grained control over the lighting conditions. We focus on the main
 159 parameters that determine the basic physical properties of light sources. The coordinates of the light
 160 source are always relative to the first frame of the video, with the camera center as the origin, and do
 161 not change as the camera moves. Except for the controllable parameters, all other intrinsic parame-
 162 ters of the light source provided by Unreal Engine 5 are completely fixed. A fixed light source refers
 163 to a light source whose parameters are always fixed during the video recording, while a variable

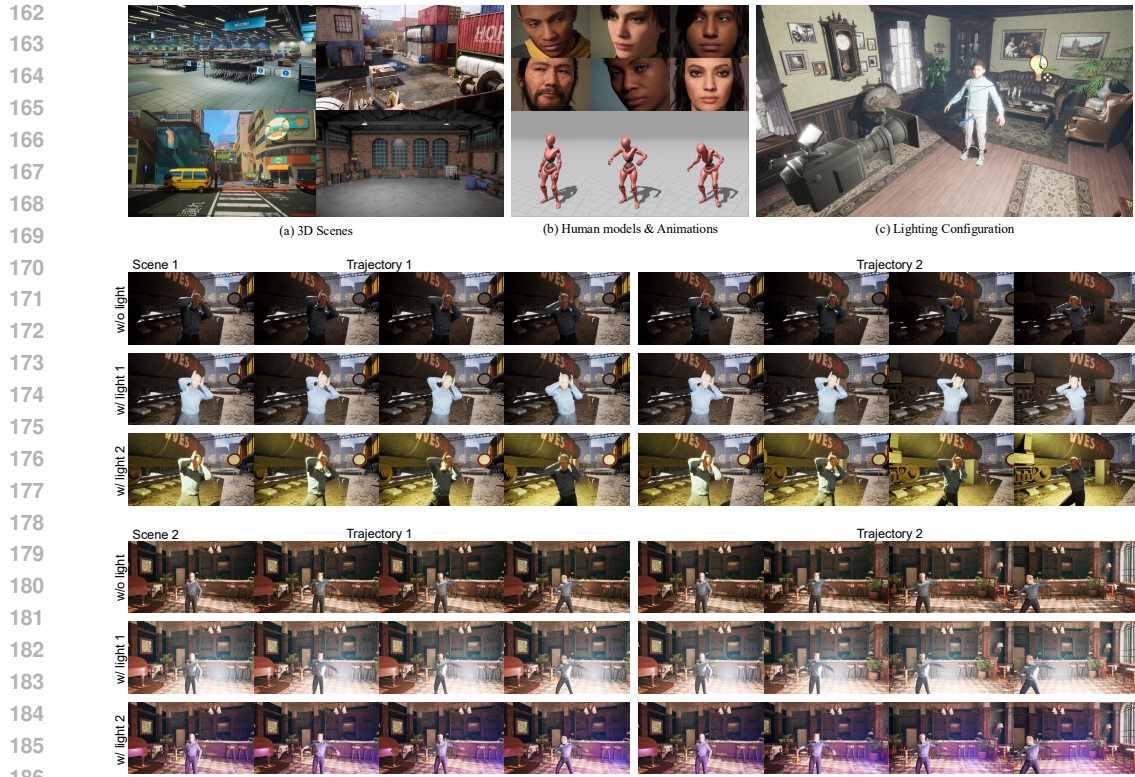


Figure 1: **Dataset Overview.** (a) and (b) show the assets used in our relighting datasets, including the 3D scenes, human models, and animations. (c) demonstrates an example lighting configuration. For each scene that has been set up, denoted as w/o light, we sample multiple camera trajectories and additional light sources to render video editing pairs with diverse motion and light conditions.

light source refers to a light source whose parameters can change over time. We develop a simple rule to generate three batches of random data to enhance data diversity. 1) Fixed light source with a fixed depth slightly behind the camera’s initial position. 2) Fixed light source with fully random parameters. 3) Variable light source with fully random parameters, and one of these parameters can further change over time. e.g., 2D coordinates, depth, color, or intensity.

We obtained a total of 7,824 pairs of training data through Unreal Engine 5 rendering, including the original video, the target video, and the corresponding original parameters of the lighting conditions. Each video has a resolution of 384x672 and a total of 77 frames. The prompts are generated based on the original videos using a common video caption model to eliminate the influence of the text content on lighting control. During the training process, the T2V base model can only generate target videos based on the given lighting conditions.

4 METHOD

A point light source contains three attributes: position $\mathbf{p} \in \mathbb{R}^3$, color $\mathbf{c} \in \mathbb{R}^3$, and intensity $I \in \mathbb{R}$. Considering that the light source may change over time, we also need a representation for temporally-varying lights. An intuitive solution to represent light sources is text, but precise lighting editing via text is difficult, as pretrained text-to-video (T2V) models have never seen such captions. Motivated by the Multi-plane Image (MPI) representing a 3D scene via multiple images at different depths, we propose a novel Multi-plane Light Image to encode 3D light information in a scene, including positions, colors, and intensities of multiple light sources. Specifically, we use 4 light images in an MPLI and compress the 4 images into one video latent feature via Video VAE, which is injected into DIT through a Light Image Adapter (LIA). For an input video of $4N + 1$ frames, we use N MPLIs to represent temporally-varying scene lighting, which naturally aligns with the pretrained DIT (Peebles & Xie, 2023). We first brief on the preliminary knowledge of the pretrained T2V model, and then elaborate on our proposed MPLI and LIA.

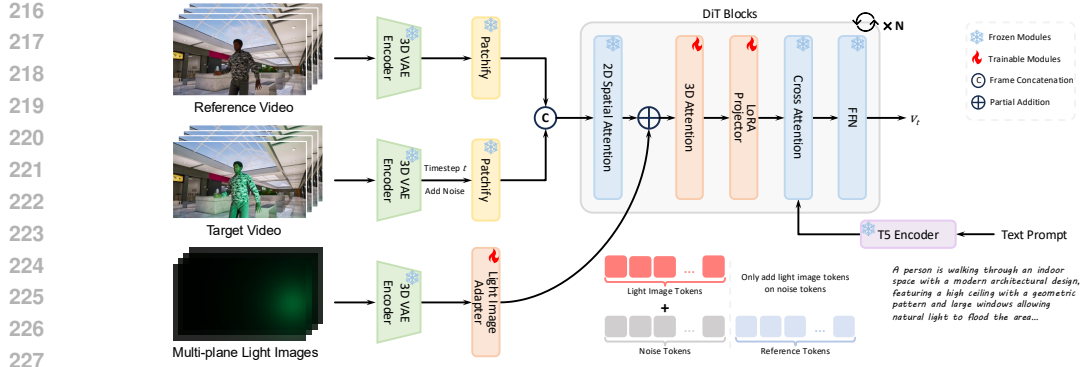


Figure 2: **An overview of our relighting training framework.** A Multi-plane Light Image (MPI) contains 4 light images, and each MPI is encoded as a latent light feature by the Video VAE. N latent light features are passed to the DiT model via our proposed Light Image Adapter (LIA), which is initialized by the pretrained patchify module and shared across different DiT blocks. The original video and the noise are temporally concatenated. The parameters of the pretrained DiT model are frozen except the 3D attention layers. We also add a LoRA module after the 3D attention layer to learn the additional editing knowledge.

4.1 PRELIMINARY

We finetune our RelightMaster on a pretrained internal text-to-video (T2V) generation model, which adopts a latent video generation architecture. Given a video with $4N + 1$ frames, the T2V model pads 3 dummy images to the video and compresses 4 images as a latent video feature via a video variational encoder (VAE) (Kingma & Welling, 2013). Then the model is trained by the conditional flow matching loss (Lipman et al., 2022). We obtain the noisy video feature $x_t = (1-t)x_0 + t\epsilon$ at the timestep t by interpolating the clean video latent feature x_0 and a noise sampled from the standard Gaussian distribution $\epsilon \in \mathcal{N}(0, 1)$ according to the timestep t , which corresponds to the ordinary differential equation (ODE): $dx_t = v_\Theta(x_t, t)dt$. The T2V model predicts the velocity $v_\Theta(x_t, t)$:

$$\mathcal{L}_{FM} = \mathbb{E}_{t, x_0, \epsilon} \|v_\Theta(x_t, t) - u_t(x_0 | \epsilon)\|_2^2. \quad (1)$$

In the inference stage, the T2V model uses the Euler scheduler to generate a video from noise:

$$x_t = x_{t-1} + v_\Theta(x_{t-1}, t) \cdot \Delta t. \quad (2)$$

t iterates from 0 to 1.

4.2 MULTI-PLANE LIGHT IMAGE REPRESENTATION

Compared to environment maps that only characterize ambient light captured from real environments, our goal is to re-light the environment with new light sources in the 3D scene, which requires accurately injecting the 3D positions of the newly added light sources into the video generation network. Inspired by Multi-Plane Image (MPI), which uses multiple images at different depths to represent 3D scenes, we propose a Multi-Plane Light Image (MPI) representation to encode the 3D positions of point light sources. Below, we first introduce the basic concept of a Light Image and then extend it to the multi-plane form.

Light Image. A Light Image is a normalized irradiance image rendered from light sources. Specifically, we place a plane orthogonal to the camera’s orientation and pass through the camera’s optical center, with a depth of d . Each pixel (x, y) on this plane corresponds to the 3D position $\mathbf{q} = (x, y, d)$ in the camera coordinate system. To simplify modeling, we approximate the point light source as a single luminous particle with an illumination intensity of I , and its 3D position in the camera coordinate system is $\mathbf{p}_l = (x_l, y_l, z_l)$. In a homogeneous medium, the luminous intensity follows the inverse-square law: the intensity at a distance r from the light source is inversely proportional to the square of r , i.e., $I_r \propto 1/r^2$. Thus, the irradiance at pixel on the Light Image is simplified as: $I_{x,y} = \frac{I}{\|\mathbf{q} - \mathbf{p}_l\|_2^2}$. To align with the video resolution, we crop an $H \times W$ region centered on the camera’s optical center from the photosensitive plane. Suppose there are multiple light sources, we

270 sum up all the irradiance to obtain the entire information. Additionally, to adjust the numerical range
 271 of irradiance for better adaptation to the video generation network, we introduce two scalers s_1 and
 272 s_2 to modify the above equation:
 273

$$274 \quad I_{x,y} = \sum_i \frac{I_i \cdot \mathbf{c}_i}{\|\mathbf{q} - \mathbf{p}_i\|_2^2 / s_1 + s_2}. \quad (3)$$

$$275$$

$$276$$

277 i indicates the i -th light source. The final RGB lighting information captured on the light image is
 278 obtained by multiplying the irradiance I_i with the color of the point light source \mathbf{c}_i .
 279

280 **Multi-Plane Light Image.** The single-plane light image can only encode the projection of light
 281 sources onto a fixed depth plane, failing to distinguish the 3D depth of different point light sources.
 282 To address this, we extend the single photosensitive plane to multiple parallel photosensitive planes
 283 as the Multi-Plane Light Image (MPLI), where each plane corresponds to a unique depth in the
 284 camera coordinate system. In our experiments, we set up four parallel photosensitive layers, each
 285 with a distinct depth. We use multiple MPLIs to further support light sources varying over time.
 286 Each MPLI corresponds to a video moment. Sequentially arranged, these MPLIs accurately capture
 287 dynamic changes (position, intensity) and meet video generation’s lighting coherence needs.
 288

289 4.3 LIGHT IMAGE ADAPTER

290 To enable effective injection of Multi-plane Light Image (MPLI), which efficiently encodes multi-
 291 source lighting in scenes, into the pre-trained text-to-video (T2V) pipeline, we further propose a
 292 Light Image Adapter (LIA). Our pre-trained T2V model processes videos with $4N + 1$ frames: after
 293 padding 3 dummy frames, a video Variational Autoencoder (VAE) compresses every 4 consecutive
 294 frames into a single video latent feature. To align with this architectural design, we set $K = 4$ for
 295 MPLI, such that a single MPLI can be compressed by the same pre-trained Video VAE into a latent
 296 light feature, matching the dimensionality and distribution of video latents. To support temporally-
 297 varying lighting, i.e., light sources varying across video frames, we associate one MPLI with each
 298 4-frame interval in the input video. Thus, for a video undergoing relighting, we configure N MPLIs
 299 in total. While this lighting representation operates at a 4-frame granularity rather than per-frame,
 300 we find it sufficient for most scenarios, since the Diffusion Transformer (DiT) model inherently
 301 smooths lighting effects for intermediate frames.

302 We propose LIA to inject sequential MPLIs into the network while preserving the pre-learned video
 303 prior. Specifically, the pre-trained T2V model first passes video latent features through a patchify
 304 module for further compression. To ensure compatibility with the learn video prior to the T2V
 305 model, our LIA reuses the structure of the patchify module and initializes its parameters with those
 306 of the pre-trained patchify module. After encoding the latent light feature, the LIA injects this
 307 signal into each DiT block. Critically, LIA parameters are shared across all blocks. We find this
 308 parameter-sharing mechanism, which plays as a form of self-regularization, crucial, as it mitigates
 309 overfitting, which is an issue that frequently arises when introducing new control modalities without
 310 such regularization. Besides LIA, we finetune the 3D attention in the pretrained T2V model to
 311 accommodate the increased token sequence length and add a low rank (LoRA) projector to absorb
 312 the additional lighting knowledge.

313 5 EXPERIMENTS

314 In this section, we first provide a series of experiments to show the controllability of our RelightMaster,
 315 and then we compare our RelightMaster with other state-of-the-art video relighting methods to
 316 show the superiority. Finally, we present ablation studies to show the effectiveness of our proposed
 317 Multi-plane Light Image and Light Image Adapter.
 318

320 5.1 CONTROLLABLE VIDEO RELIGHTING

321 To comprehensively evaluate the effectiveness of our proposed RelightMaster in handling diverse
 322 lighting conditions for video relighting, we design a series of controlled experiments. Our Relight-
 323 Master generates relit videos according to the input lighting conditions, which include light source

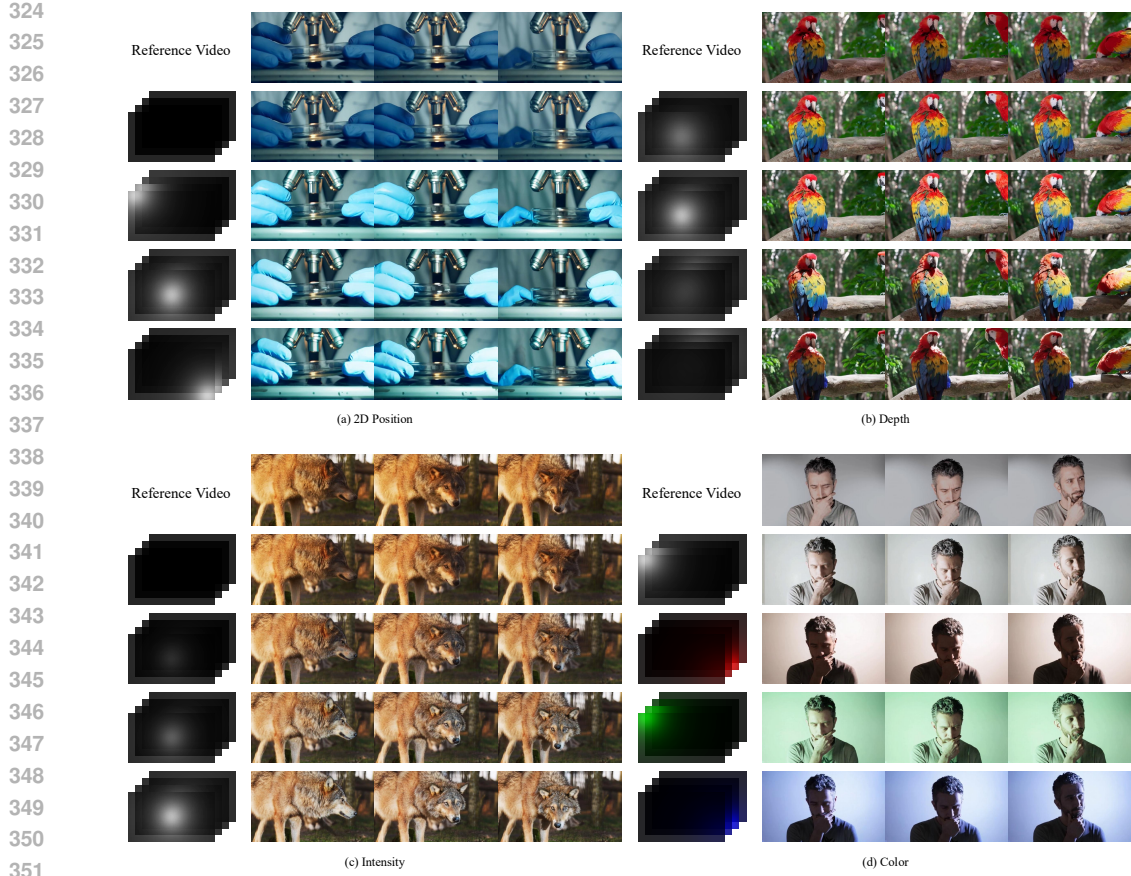


Figure 3: **Relighting with fixed light source.** (a) and (b) demonstrate the light source position, (c) reflects the light source intensity, and (d) indicates the light color.

positions in the 3D camera frustum, and the light color and intensity. We thus individually control the light conditions and relight the query videos in Fig. 3 to demonstrate precise controllability.

Light source position. We conduct two experiments that correspond to Fig. 3 (a) and (b), respectively. In experiment (a), we use a baseline video with no additional light sources to preserve the original appearance of the input video. We then compare this baseline against relit videos that use a single point light source with fixed depth. This point light source is placed at three distinct 2D positions: top-left, center, and bottom-right. The relit videos exhibit position-dependent specular reflections. Specifically, visible highlight regions appear on the rubber gloves of the dynamic object, and these highlights align with the 2D positions of the applied light sources. In experiment (b), we fix the 2D position of the point light source to the center and then gradually increase the depth of the light source. We generate four relit videos with increasing depth values, and each video shows distinct lighting effects. The shallow depth produces frontal low-intensity illumination. The moderate depth creates side illumination, and the large depth, with the light source behind the scarlet macaw, results in backlighting. These results confirm that the model accurately responds to adjustments in light source position, enabling fine-grained control over 3D lighting position.

Light intensity. In Fig. 3 (c), we fix the 3D position of a white point light source and gradually increase the light intensity starting from 0, equivalent to no additional light, to higher values, generating a sequence of relit videos with incremental intensity levels. The relit videos exhibit a clear correlation with the increasing light intensity. The wolf’s head and body are gradually brightened by the white light as the intensity rises. Concurrently, the cast shadows also become progressively stronger with higher intensity. Such lighting effects reflect the model’s accurate response to light intensity adjustments.

Light color and position. In this experiment, we fix the 3D position of the point light source to a side-lighting configuration and keep its intensity constant at a moderate level to avoid overexposure. We then test four distinct light colors: white, red, green, and blue, generating a separate relit video

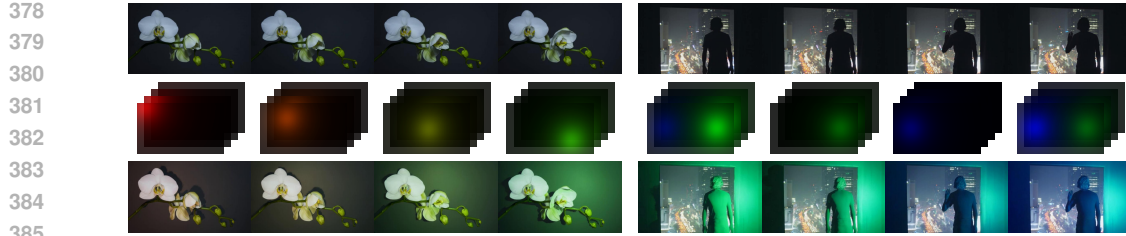


Figure 4: **Relighting with temporally-varying lights and multi-lights.** Our RelightMaster supports multiple and temporally-varying light source control. The corresponding Multi-plane Light Images (MPLI) at different moments are visualized for better understanding.

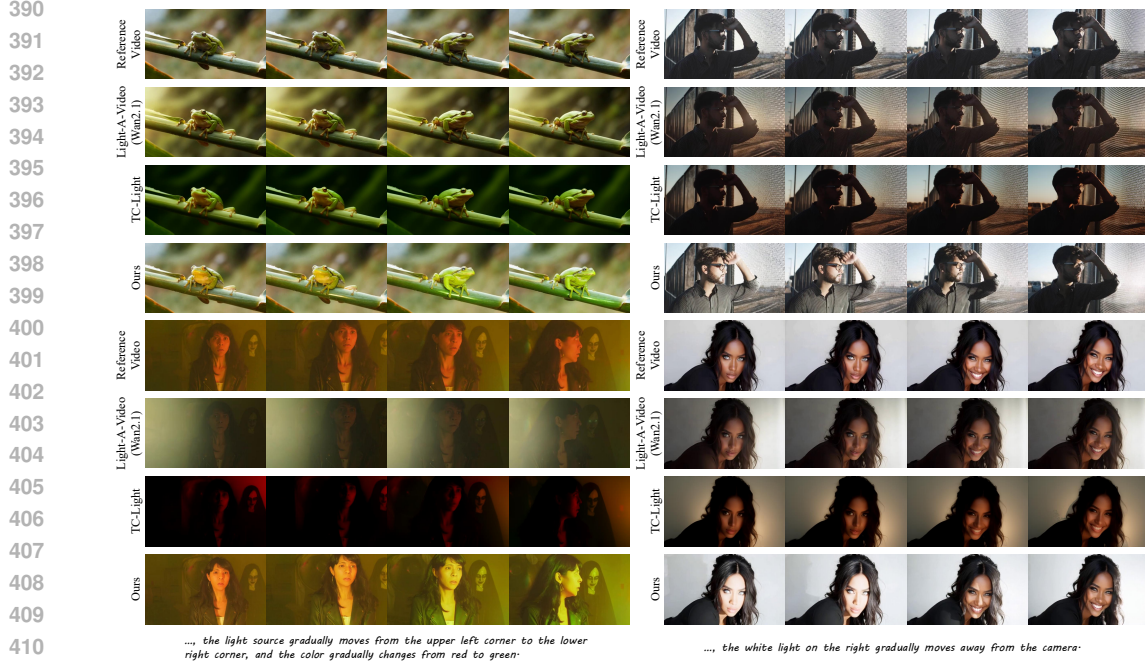


Figure 5: **Comparison with other video relighting methods.** We translate our precise light control signals to text and feed them to Light-A-Video (Zhou et al., 2025) and TC-Light (Zhou et al., 2025) for each color. As shown in Fig. 3 (d), each relit video exhibits color-specific lighting effects that align with the applied light color. Specifically, on the male subject in the video, the face, hair, and clothing folds all show corresponding color-cast. Moreover, across all color settings, natural shadows, which are consistent with the side-lighting position, and diffuse reflections are clearly observed. These natural and color-accurate lighting effects reflect the precise color control capability.

Temporally-varying lights and multi-lights. In Fig. 4, over the duration of the video corresponding to the flower, we apply two temporal variations: 1) the light source moves continuously from the top-left to the bottom-right and 2) the light color transitions smoothly from red to green. As observed in the relit video, the flower’s petals and stamens show color casts shifting from red to green, while the highlight and shadow positions on the flower surface follow the light’s movement. For the video of the man, we deploy a blue light and a green light in the scene. We make the blue light intensity stronger and the green light weaker. The relit video accurately responds to the light variations. These results denote that our RelightMaster can precisely synchronize temporal adjustments of light position and color and support multiple lights.

5.2 COMPARISON WITH STATE-OF-THE-ART VIDEO RELIGHTING

We choose Light-A-Video (Zhou et al., 2025) and TC-Light (Liu et al., 2025b) for comparison. Light-A-Video and TC-Light extend the light control capability of IC-Light (Zhang et al., 2024)



Figure 6: Generalization to multi-lights.



Figure 7: Light Image Adapter Initialization. “zero init” and “copy init” respectively denote that the LIA is initialized with a zero convolution or the parameters from the pretrained patchifier.

from images to videos. Similar to IC-Light, they rely on text prompts and an environment map to regulate relighting effects. However, the use of an environment map will replace the background of the original image or video, which is unacceptable for scenarios requiring background preservation. We thus transform the relighting conditions into text descriptions and append these descriptions to the original video caption and feed the merged prompt to Light-A-Video to obtain its relighting results. For our RelightMaster, we use the Multi-plane Light Images (MPLI) to indicate the relighting conditions. We conduct four experiments for comparison, as shown in Fig. 5. Two experiments focus on dynamic light position and color changes: the light source is moved from the top-left to the bottom-right of the frame, with its color gradually transitioning from red to green. The remaining two groups involve dynamic depth adjustment of a white light source, which is gradually moved forward along the camera lens. We compare our RelightMaster against Light-A-Video and TC-Light to reveal the clear performance gaps. Light-A-Video and TC-Light show no response to the relighting conditions. In contrast, our RelightMaster accurately responds to the instructions. In the position-color transition experiments, the light source moves smoothly from the top-left to the bottom-right, with the color gradually shifting from red to green. In the other experiments where the white light source moves forward, a dynamic and physically consistent lighting process is observed on the male and female subjects: initially, the white light brightens them by direct illumination. As the light continues to advance past the subjects’ lateral position, the subjects begin to be partially occluded by their own contours, resulting in subtle shadow. Finally, the light moves further forward to the back of the object. The subjects exhibit a clear backlighting effect, indicating that our RelightMaster clearly outperforms the other methods.

5.3 ABLATION STUDY

We provide two ablation studies with a single Light Image, i.e., $K = 1$, and on a 1/3 training dataset. As shown in Fig. 6, trained only on the single light source relighting data, our method can generalize to multi-source light source relighting, which reveals the extraordinary generalization performance of our Light Map representation. A common strategy used in image and video adapters is to initialize the parameters with a zero-convolution. However, the zero-initialization technique can not activate the relighting controllability (Fig. 7). In contrast, we initialize our Light Image Adapter with the parameters from the patchifier enabling video relighting, which reveals the significance that aligns the lighting control signals to the prior distribution learned by the DiT.

6 CONCLUSION

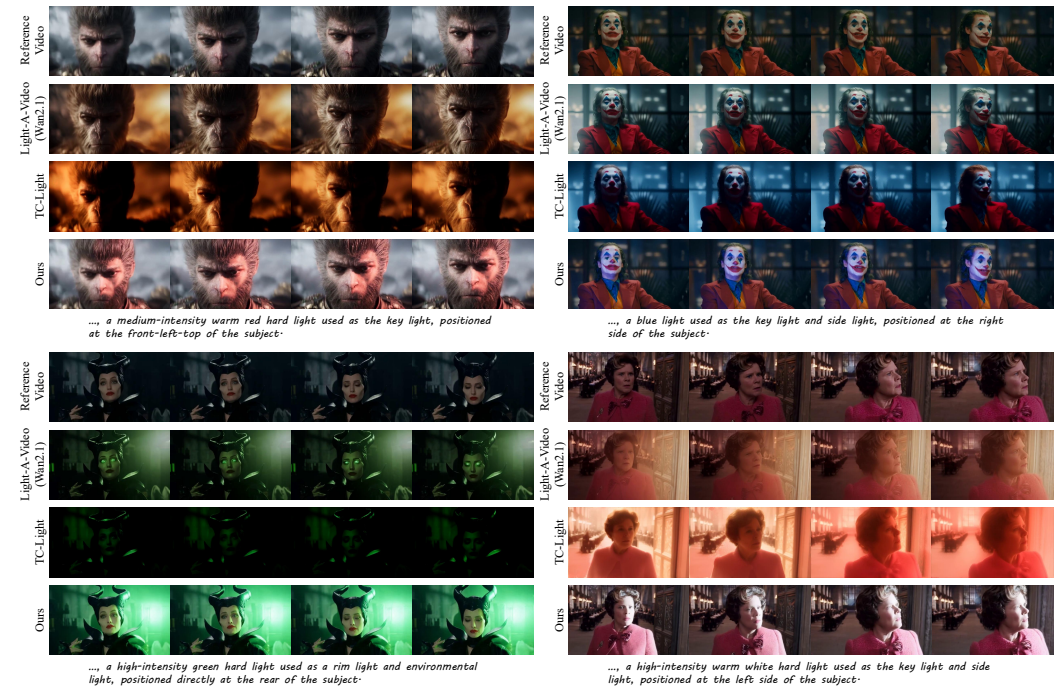
We proposed a novel framework RelightMaster for video relighting, which includes a dataset RelightVideo, a Multi-plane Light Image (MPLI) for accurate light source control, and a Light Image Adapter (LIA) for light feature injection. The experiments demonstrated that RelightMaster is able to individually control the light source position, color, and intensity for video relighting.

486 REFERENCES
487

- 488 Jianhong Bai, Menghan Xia, Xiao Fu, Xintao Wang, Lianrui Mu, Jinwen Cao, Zuozhu Liu, Haoji
489 Hu, Xiang Bai, Pengfei Wan, et al. Recammaster: Camera-controlled generative rendering from
490 a single video. *arXiv preprint arXiv:2503.11647*, 2025.
- 491 Weikang Bian, Zhaoyang Huang, Xiaoyu Shi, Yijin Li, Fu-Yun Wang, and Hongsheng Li. Gs-
492 dit: Advancing video generation with pseudo 4d gaussian fields through efficient dense 3d point
493 tracking. *arXiv preprint arXiv:2501.02690*, 2025.
- 494 Andreas Blattmann, Tim Dockhorn, Sumith Kulal, Daniel Mendelevitch, Maciej Kilian, Dominik
495 Lorenz, Yam Levi, Zion English, Vikram Voleti, Adam Letts, et al. Stable video diffusion: Scaling
496 latent video diffusion models to large datasets. *arXiv preprint arXiv:2311.15127*, 2023.
- 497 Jiazi Bu, Pengyang Ling, Pan Zhang, Tong Wu, Xiaoyi Dong, Yuhang Zang, Yuhang Cao, Dahua
498 Lin, and Jiaqi Wang. Broadway: Boost your text-to-video generation model in a training-free
499 way. *arXiv preprint arXiv:2410.06241*, 2024.
- 500 Chris Careaga and Yağız Aksoy. Intrinsic image decomposition via ordinal shading. *ACM Transac-
501 tions on Graphics*, 43(1):1–24, 2023.
- 502 Jiaxin Cheng, Tianjun Xiao, and Tong He. Consistent video-to-video transfer using synthetic dataset.
503 *arXiv preprint arXiv:2311.00213*, 2023.
- 504 Prafulla Dhariwal and Alexander Nichol. Diffusion models beat gans on image synthesis. *Advances
505 in neural information processing systems*, 34:8780–8794, 2021.
- 506 Ye Fang, Zeyi Sun, Shangzhan Zhang, Tong Wu, Yinghao Xu, Pan Zhang, Jiaqi Wang, Gordon
507 Wetzstein, and Dahua Lin. Relightvid: Temporal-consistent diffusion model for video relighting.
508 *arXiv preprint arXiv:2501.16330*, 2025.
- 509 Epic Games. Unreal engine 5. [https://www.unrealengine.com/en-US/
510 unreal-engine-5](https://www.unrealengine.com/en-US/unreal-engine-5), 2022.
- 511 Zekai Gu, Rui Yan, Jiahao Lu, Peng Li, Zhiyang Dou, Chenyang Si, Zhen Dong, Qifeng Liu, Cheng
512 Lin, Ziwei Liu, et al. Diffusion as shader: 3d-aware video diffusion for versatile video generation
513 control. In *Proceedings of the Special Interest Group on Computer Graphics and Interactive
514 Techniques Conference Conference Papers*, pp. 1–12, 2025.
- 515 Hao He, Ceyuan Yang, Shanchuan Lin, Yinghao Xu, Meng Wei, Liangke Gui, Qi Zhao, Gordon
516 Wetzstein, Lu Jiang, and Hongsheng Li. Cameractrl ii: Dynamic scene exploration via camera-
517 controlled video diffusion models. *arXiv preprint arXiv:2503.10592*, 2025.
- 518 Jonathan Ho, Ajay Jain, and Pieter Abbeel. Denoising diffusion probabilistic models. *Advances in
519 neural information processing systems*, 33:6840–6851, 2020.
- 520 Diederik P Kingma and Max Welling. Auto-encoding variational bayes. *arXiv preprint
521 arXiv:1312.6114*, 2013.
- 522 Peter Kocsis, Julien Philip, Kalyan Sunkavalli, Matthias Nießner, and Yannick Hold-Geoffroy.
523 Lightit: Illumination modeling and control for diffusion models. In *Proceedings of the IEEE/CVF
524 Conference on Computer Vision and Pattern Recognition*, pp. 9359–9369, 2024.
- 525 Max Ku, Cong Wei, Weiming Ren, Huan Yang, and Wenhui Chen. Anyv2v: A tuning-free framework
526 for any video-to-video editing tasks. *Transactions on Machine Learning Research*, 2024.
- 527 Zhihao Liang, Hongdong Li, Kui Jia, Kailing Guo, and Qi Zhang. Gus-ir: Gaussian splatting
528 with unified shading for inverse rendering. *IEEE Transactions on Pattern Analysis and Machine
529 Intelligence*, 2025.
- 530 Pengyang Ling, Jiazi Bu, Pan Zhang, Xiaoyi Dong, Yuhang Zang, Tong Wu, Huaian Chen, Jiaqi
531 Wang, and Yi Jin. Motionclone: Training-free motion cloning for controllable video generation.
532 *arXiv preprint arXiv:2406.05338*, 2024.

- 540 Yaron Lipman, Ricky TQ Chen, Heli Ben-Hamu, Maximilian Nickel, and Matt Le. Flow matching
 541 for generative modeling. *arXiv preprint arXiv:2210.02747*, 2022.
 542
- 543 Lijie Liu, Tianxiang Ma, Bingchuan Li, Zhuowei Chen, Jiawei Liu, Gen Li, Siyu Zhou, Qian He,
 544 and Xinglong Wu. Phantom: Subject-consistent video generation via cross-modal alignment.
 545 *arXiv preprint arXiv:2502.11079*, 2025a.
- 546 Yang Liu, Chuanchen Luo, Zimo Tang, Yingyan Li, Yuran Yang, Yuanyong Ning, Lue Fan, Junran
 547 Peng, and Zhaoxiang Zhang. Tc-light: Temporally consistent relighting for dynamic long videos.
 548 *arXiv preprint arXiv:2506.18904*, 2025b.
- 549 Jundan Luo, Zhaoyang Huang, Yijin Li, Xiaowei Zhou, Guofeng Zhang, and Hujun Bao. Niid-net:
 550 Adapting surface normal knowledge for intrinsic image decomposition in indoor scenes. *IEEE*
 551 *Transactions on Visualization and Computer Graphics*, 26(12):3434–3445, 2020.
- 552 Nadav Magar, Amir Hertz, Eric Tabellion, Yael Pritch, Alex Rav-Acha, Ariel Shamir, and Yedid
 553 Hoshen. Lightlab: Controlling light sources in images with diffusion models. In *Proceedings of*
 554 *the Special Interest Group on Computer Graphics and Interactive Techniques Conference Con-*
 555 *ference Papers*, pp. 1–11, 2025.
- 556 William Peebles and Saining Xie. Scalable diffusion models with transformers. In *Proceedings of*
 557 *the IEEE/CVF international conference on computer vision*, pp. 4195–4205, 2023.
- 558
- 559 Robin Rombach, Andreas Blattmann, Dominik Lorenz, Patrick Esser, and Björn Ommer. High-
 560 resolution image synthesis with latent diffusion models. In *Proceedings of the IEEE/CVF confer-*
 561 *ence on computer vision and pattern recognition*, pp. 10684–10695, 2022.
- 562 Uriel Singer, Amit Zohar, Yuval Kirstain, Shelly Sheynin, Adam Polyak, Devi Parikh, and Yaniv
 563 Taigman. Video editing via factorized diffusion distillation. In *European Conference on Computer*
 564 *Vision*, pp. 450–466. Springer, 2025.
- 565
- 566 Jiaming Song, Chenlin Meng, and Stefano Ermon. Denoising diffusion implicit models. *arXiv*
 567 *preprint arXiv:2010.02502*, 2020.
- 568
- 569 Richard Tucker and Noah Snavely. Single-view view synthesis with multiplane images. In *Proceed-
 570 ings of the IEEE/CVF Conference on Computer Vision and Pattern Recognition*, pp. 551–560,
 571 2020.
- 572
- 573 Team Wan, Ang Wang, Baole Ai, Bin Wen, Chaojie Mao, Chen-Wei Xie, Di Chen, Feiwu Yu,
 574 Haiming Zhao, Jianxiao Yang, Jianyuan Zeng, Jiayu Wang, Jingfeng Zhang, Jingren Zhou, Jinkai
 575 Wang, Jixuan Chen, Kai Zhu, Kang Zhao, Keyu Yan, Lianghua Huang, Mengyang Feng, Ningyi
 576 Zhang, Pandeng Li, Pingyu Wu, Ruihang Chu, Ruili Feng, Shiwei Zhang, Siyang Sun, Tao Fang,
 577 Tianxing Wang, Tianyi Gui, Tingyu Weng, Tong Shen, Wei Lin, Wei Wang, Wei Wang, Wenmeng
 578 Zhou, Wente Wang, Wenting Shen, Wenyuan Yu, Xianzhong Shi, Xiaoming Huang, Xin Xu, Yan
 579 Kou, Yangyu Lv, Yifei Li, Yijing Liu, Yiming Wang, Yingya Zhang, Yitong Huang, Yong Li, You
 580 Wu, Yu Liu, Yulin Pan, Yun Zheng, Yuntao Hong, Yupeng Shi, Yutong Feng, Zeyinzi Jiang, Zhen
 581 Han, Zhi-Fan Wu, and Ziyu Liu. Wan: Open and advanced large-scale video generative models.
arXiv preprint arXiv:2503.20314, 2025.
- 582
- 583 Jay Zhangjie Wu, Yixiao Ge, Xintao Wang, Stan Weixian Lei, Yuchao Gu, Wynne Hsu, Ying Shan,
 584 Xiaohu Qie, and Mike Zheng Shou. Tune-a-video: One-shot tuning of image diffusion models
 585 for text-to-video generation. arxiv 2022. *arXiv preprint arXiv:2212.11565*, 2022.
- 586
- 587 Chong Zeng, Yue Dong, Pieter Peers, Youkang Kong, Hongzhi Wu, and Xin Tong. Dilightnet:
 588 Fine-grained lighting control for diffusion-based image generation. In *ACM SIGGRAPH 2024*
 589 *Conference Papers*, pp. 1–12, 2024.
- 590
- 591 Jianshu Zeng, Yuxuan Liu, Yutong Feng, Chenxuan Miao, Zixiang Gao, Jiwang Qu, Jianzhang
 592 Zhang, Bin Wang, and Kun Yuan. Lumen: Consistent video relighting and harmonious back-
 593 ground replacement with video generative models. *arXiv preprint arXiv:2508.12945*, 2025.
- 594
- 595 Lvmin Zhang, Anyi Rao, and Maneesh Agrawala. Ic-light github page. <https://github.com/lvminzhang/IC-Light>, 2024.

594 Yujie Zhou, Jiazi Bu, Pengyang Ling, Pan Zhang, Tong Wu, Qidong Huang, Jinsong Li, Xiaoyi
595 Dong, Yuhang Zang, Yuhang Cao, et al. Light-a-video: Training-free video relighting via pro-
596 gressive light fusion. *arXiv preprint arXiv:2502.08590*, 2025.
597
598
599
600
601
602
603
604
605
606
607
608
609
610
611
612
613
614
615
616
617
618
619
620
621
622
623
624
625
626
627
628
629
630
631
632
633
634
635
636
637
638
639
640
641
642
643
644
645
646
647

648
649
A APPENDIX650
651
LLM usage. We used Gemini to help us polish our writing.675
676
677
678
Figure 8: Visualization for the quantitative comparison679
680
681
Table 1: Quantitative Comparison on Synthetic Dataset

METHOD	PSNR \uparrow	SSIM \uparrow	LPIPS \downarrow
Light-A-Video	12.984	0.621	0.338
TC-Light	10.534	0.432	0.525
Ours	19.456	0.808	0.157

685
686
687
688
Table 2: Quantitative comparison on Real Videos with VBench Metrics

METHOD	Subject Consistency \uparrow	Background Consistency \uparrow	Motion Smoothness \uparrow	Dynamic Degree \uparrow	Aesthetic Quality \uparrow	Imaging Quality \uparrow
Light-A-Video	0.960	0.972	0.993	0.4	0.604	0.479
TC-Light	0.953	0.961	0.996	0.4	0.549	0.351
Ours	0.958	0.972	0.994	0.4	0.598	0.612

696
697
Quantitative Comparison on Synthetic Dataset To enable a direct comparison against Ground
698
699
700
701
702
703
704
705
706
707
708
709
710
711
712
713
714
715
716
717
718
719
720
721
722
723
724
725
726
727
728
729
730
731
732
733
734
735
736
737
738
739
740
741
742
743
744
745
746
747
748
749
750
751
752
753
754
755
756
757
758
759
760
761
762
763
764
765
766
767
768
769
770
771
772
773
774
775
776
777
778
779
780
781
782
783
784
785
786
787
788
789
790
791
792
793
794
795
796
797
798
799
800
801
802
803
804
805
806
807
808
809
8010
8011
8012
8013
8014
8015
8016
8017
8018
8019
8020
8021
8022
8023
8024
8025
8026
8027
8028
8029
8030
8031
8032
8033
8034
8035
8036
8037
8038
8039
8040
8041
8042
8043
8044
8045
8046
8047
8048
8049
8050
8051
8052
8053
8054
8055
8056
8057
8058
8059
8060
8061
8062
8063
8064
8065
8066
8067
8068
8069
8070
8071
8072
8073
8074
8075
8076
8077
8078
8079
8080
8081
8082
8083
8084
8085
8086
8087
8088
8089
8090
8091
8092
8093
8094
8095
8096
8097
8098
8099
80100
80101
80102
80103
80104
80105
80106
80107
80108
80109
80110
80111
80112
80113
80114
80115
80116
80117
80118
80119
80120
80121
80122
80123
80124
80125
80126
80127
80128
80129
80130
80131
80132
80133
80134
80135
80136
80137
80138
80139
80140
80141
80142
80143
80144
80145
80146
80147
80148
80149
80150
80151
80152
80153
80154
80155
80156
80157
80158
80159
80160
80161
80162
80163
80164
80165
80166
80167
80168
80169
80170
80171
80172
80173
80174
80175
80176
80177
80178
80179
80180
80181
80182
80183
80184
80185
80186
80187
80188
80189
80190
80191
80192
80193
80194
80195
80196
80197
80198
80199
80200
80201
80202
80203
80204
80205
80206
80207
80208
80209
80210
80211
80212
80213
80214
80215
80216
80217
80218
80219
80220
80221
80222
80223
80224
80225
80226
80227
80228
80229
80230
80231
80232
80233
80234
80235
80236
80237
80238
80239
80240
80241
80242
80243
80244
80245
80246
80247
80248
80249
80250
80251
80252
80253
80254
80255
80256
80257
80258
80259
80260
80261
80262
80263
80264
80265
80266
80267
80268
80269
80270
80271
80272
80273
80274
80275
80276
80277
80278
80279
80280
80281
80282
80283
80284
80285
80286
80287
80288
80289
80290
80291
80292
80293
80294
80295
80296
80297
80298
80299
80300
80301
80302
80303
80304
80305
80306
80307
80308
80309
80310
80311
80312
80313
80314
80315
80316
80317
80318
80319
80320
80321
80322
80323
80324
80325
80326
80327
80328
80329
80330
80331
80332
80333
80334
80335
80336
80337
80338
80339
80340
80341
80342
80343
80344
80345
80346
80347
80348
80349
80350
80351
80352
80353
80354
80355
80356
80357
80358
80359
80360
80361
80362
80363
80364
80365
80366
80367
80368
80369
80370
80371
80372
80373
80374
80375
80376
80377
80378
80379
80380
80381
80382
80383
80384
80385
80386
80387
80388
80389
80390
80391
80392
80393
80394
80395
80396
80397
80398
80399
80400
80401
80402
80403
80404
80405
80406
80407
80408
80409
80410
80411
80412
80413
80414
80415
80416
80417
80418
80419
80420
80421
80422
80423
80424
80425
80426
80427
80428
80429
80430
80431
80432
80433
80434
80435
80436
80437
80438
80439
80440
80441
80442
80443
80444
80445
80446
80447
80448
80449
80450
80451
80452
80453
80454
80455
80456
80457
80458
80459
80460
80461
80462
80463
80464
80465
80466
80467
80468
80469
80470
80471
80472
80473
80474
80475
80476
80477
80478
80479
80480
80481
80482
80483
80484
80485
80486
80487
80488
80489
80490
80491
80492
80493
80494
80495
80496
80497
80498
80499
80500
80501
80502
80503
80504
80505
80506
80507
80508
80509
80510
80511
80512
80513
80514
80515
80516
80517
80518
80519
80520
80521
80522
80523
80524
80525
80526
80527
80528
80529
80530
80531
80532
80533
80534
80535
80536
80537
80538
80539
80540
80541
80542
80543
80544
80545
80546
80547
80548
80549
80550
80551
80552
80553
80554
80555
80556
80557
80558
80559
80560
80561
80562
80563
80564
80565
80566
80567
80568
80569
80570
80571
80572
80573
80574
80575
80576
80577
80578
80579
80580
80581
80582
80583
80584
80585
80586
80587
80588
80589
80590
80591
80592
80593
80594
80595
80596
80597
80598
80599
80600
80601
80602
80603
80604
80605
80606
80607
80608
80609
80610
80611
80612
80613
80614
80615
80616
80617
80618
80619
80620
80621
80622
80623
80624
80625
80626
80627
80628
80629
80630
80631
80632
80633
80634
80635
80636
80637
80638
80639
80640
80641
80642
80643
80644
80645
80646
80647
80648
80649
80650
80651
80652
80653
80654
80655
80656
80657
80658
80659
80660
80661
80662
80663
80664
80665
80666
80667
80668
80669
80670
80671
80672
80673
80674
80675
80676
80677
80678
80679
80680
80681
80682
80683
80684
80685
80686
80687
80688
80689
80690
80691
80692
80693
80694
80695
80696
80697
80698
80699
80700
80701
80702
80703
80704
80705
80706
80707
80708
80709
80710
80711
80712
80713
80714
80715
80716
80717
80718
80719
80720
80721
80722
80723
80724
80725
80726
80727
80728
80729
80730
80731
80732
80733
80734
80735
80736
80737
80738
80739
80740
80741
80742
80743
80744
80745
80746
80747
80748
80749
80750
80751
80752
80753
80754
80755
80756
80757
80758
80759
80760
80761
80762
80763
80764
80765
80766
80767
80768
80769
80770
80771
80772
80773
80774
80775
80776
80777
80778
80779
80780
80781
80782
80783
80784
80785
80786
80787
80788
80789
80790
80791
80792
80793
80794
80795
80796
80797
80798
80799
80800
80801
80802
80803
80804
80805
80806
80807
80808
80809
80810
80811
80812
80813
80814
80815
80816
80817
80818
80819
80820
80821
80822
80823
80824
80825
80826
80827
80828
80829
80830
80831
80832
80833
80834
80835
80836
80837
80838
80839
80840
80841
80842
80843
80844
80845
80846
80847
80848
80849
80850
80851
80852
80853
80854
80855
80856
80857
80858
80859
80860
80861
80862
80863
80864
80865
80866
80867
80868
80869
80870
80871
80872
80873
80874
80875
80876
80877
80878
80879
80880
80881
80882
80883
80884
80885
80886
80887
80888
80889
80890
80891
80892
80893
80894
80895
80896
80897
80898
80899
80900
80901
80902
80903
80904
80905
80906
80907
80908
80909
80910
80911
80912
80913
80914
80915
80916
80917
80918
80919
80920
80921
80922
80923
80924
80925
80926
80927
80928
80929
80930
80931
80932
80933
80934
80935
80936
80937
80938
80939
80940
80941
80942
80943
80944
80945
80946
80947
80948
80949
80950
80951
80952
80953
80954
80955
80956
80957
80958
80959
80960
80961
80962
80963
80964
80965
80966
80967
80968
80969
80970
80971
80972
80973
80974
80975
80976
80977
80978
80979
80980
80981
80982
80983
80984
80985
80986
80987
80988
80989
80990
80991
80992
80993
80994
80995
80996
80997
80998
80999
80100
80101
80102
80103
80104
80105
80106
80107
80108
80109
80110
80111
80112
80113
80114
80115
80116
80117
80118
80119
80120
80121
80122
80123
80124
80125
80126
80127
80128
80129
80130
80131
80132
80133
80134
80135
80136
80137
80138
80139
80140
80141
80142
80143
80144
80145
80146
80147
80148
80149
80150
80151
80152
80153
80154
80155
80156
80157
80158
80159
80160
80161
80162
80163
80164
80165
80166
80167
80168
80169
80170
80171
80172
80173
80174
80175
80176
80177
80178
80179
80180
80181
80182
80183
80184
80185
80186
80187
80188
80189
80190
80191
80192
80193
80194
80195
80196
80197
80198
80199
80200
80201
80202
80203
80204
80205
80206
80207
80208
80209
80210
80211
80212
80213
80214
80215
80216
80217
80218
80219
80220
80221
80222
80223
80224
80225
80226
80227
80228
80229
80230
80231
80232
80233
80234
80235
80236
80237
80238
80239
80240
80241
80242
80243
80244
80245
80246
80247
80248
80249
80250
80251
80252
80253
80254
80255
80256
80257
80258
80259
80260
80261
80262
80263
80264
80265
80266
80267
80268
80269
80270
80271
80272
80273
80274
80275
80276
80277
80278
80279
80280
80281
80282
80283
80284
80285
80286
80287
80288
80289
80290
80291
80292
80293
80294
80295
80296
80297
80298
80299
80300
80301
80302
80303
80304
80305
80306
80307
80308
80309
80310
80311
80312
80313
80314
80315
80316
80317
80318
80319
80320
80321
80322
80323
80324
80325
80326
80327
80328
80329
80330
80331
80332
80333
80334
80335
80336
80337
80338
80339
80340
80341
80342
80343
80344
80345
80346
80347
80348
80349
80350
80351
80352
80353
80354
80355
80356
80357
80358
80359
80360
80361
80362
80363
80364
80365
80366
80367
80368
80369
80370
80371
80372
80373
80374
80375
80376
80377
80378
80379
80380
80381
80382
80383
80384
80385
80386
80387
80388
80389
80390
80391
80392
80393
80394
80395
80396
80397
80398
80399
80400
80401
80402
80403
80404
80405
80406
80407
80408
80409
80410
80411
80412
80413
80414
80415
80416
80417
80418
80419
80420
80421
80

702

703

Table 3: Quantitative Comparison on the User Study Results

704

705

METHOD	Video Quality ↑	Relight Controllability ↑	Content retention ↑
Light-A-Video	0	2	2
TC-Light	0	0	0
Ours	130	128	128

706

707

708

709

710

711

Table 4: Ablation Study on K with Video Reconstruction Metrics.

712

713

714

715

716

717

718

K	PSNR ↑	SSIM ↑	LPIPS ↓
2	23.546	0.866	0.113
4	23.456	0.869	0.105
8	23.581	0.866	0.107

719

720

721

722

723

724

725

726

727

728

729

Quantitative Comparison on Real Videos. To evaluate performance in diverse real-world scenarios, we curated a test set comprising 10 classic clips selected from various movies. We visualized 4 of them in Fig. 8. Since GT is unavailable, we compare the performance by video generation metrics and human evaluation. We utilized VBench to assess the general video generation quality as shown in Tab. 2. The “imaging quality” metrics indicate that the quality of videos generated by our RelightMaster significantly surpasses the other two methods. Regarding the aesthetic quality metric, RelightMaster performs comparably to Light-A-Video. However, in terms of actual human perception, our method demonstrates significantly better visual quality. We attribute this discrepancy to the inherent bias in the aesthetic operator. We also conducted a user study to evaluate editing accuracy (i.e., how well the lighting change matches the prompt/control) with these 10 videos. Participants were asked to select the best results from the generated videos in terms of three questions:

730

731

732

733

- Which video presents the best quality?
- Which video presents the best relighting controllability?
- Which video best preserves the content of the input video?

734

735

736

737

738

739

740

741

742

Table 5: Ablation Study on K with VBench Metrics

743

744

745

746

747

748

749

750

751

752

753

754

755

There are 13 people participating in the user study. We collect the scores for each of the three methods across the three questions as shown in Tab. 3. The results present that our RelightMaster dominantly outperforms the other three methods. The quality of videos generated by Light-A-Video and TC-Light is not visually pleasing and the controllability is not good enough, as shown in Fig. 8. In contrast, the videos generated by our RelightMaster present good aesthetics and fine-grained controllability, which explains why most users rank videos generated by our RelightMaster 1st in the user study.

K	Subject Consistency ↑	Background Consistency ↑	Motion Smoothness ↑	Dynamic Degree ↑	Aesthetic Quality ↑	Imaging Quality ↑
2	0.930	0.939	0.993	0.563	0.538	0.602
4	0.930	0.941	0.993	0.594	0.546	0.609
8	0.929	0.939	0.993	0.594	0.534	0.611

Ablation Study on K. We provide an ablation study to show the reason why we select $K = 4$. We render 32 video pairs that contain temporally varying light sources to evaluate the performance. We compare the models with different numbers of multi-plane light maps (K) with the video reconstruction metrics in Tab. 4 and video quality metrics (VBench) in Tab. 5. We observe significant performance improvement, including LPIPS in the Tab. 4 and dynamic degree and aesthetic quality in Tab. 5, from $K = 2$ to $K = 4$, but the performance of $K = 4$ and $K = 8$ is comparable. We thus select $K = 4$ as our final setting.